Performance Comparison of Coherent and Direct Detection Schemes for 50G PON

Yixiao Zhu[1], Bo Yang[1], Yiming Zhong[1], Zheng Liu[1], Yong Guo[1], Jun Shan Wey[2], Xingang Huang[1], and Zhuang Ma[1]

ZTE Corporation, Shanghai, China[1]; ZTE(TX) Inc., Morristown, NJ 07960, USA[2]

zhu.yixiao@zte.com.cn

Abstract: We investigate various coherent and direct detection schemes with 50Gb/s/λ NRZ signal through simulation. The receiver sensitivity, the influence of frequency offset, LO power, laser linewidth, and fiber dispersion are studied for each structure.

OCIS codes: (060.2360) Fiber optics links and subsystems; (060.4252) Networks, broadcast; (060.4080) Modulation

1. Introduction

The rapid development of Internet of Things, 4K/8K high-definition video, and other broadband services has put forward higher bandwidth requirements for access network. Recently, the IEEE 802.3ca Task Force is finalizing 25/50G EPON standards [1], while ITU-T Q2/SG15 has also begun the standardization process of a series of Recommendations including a single wavelength 50G-PON [2]. To support high power budget, one way is to use avalanche photodiode (APD) or the combination of semiconductor optical amplifier (SOA) and positive-intrinsic-negative (pin) PD [3] as DD receiver. Alternately, coherent detection (CD) has also been demonstrated as a promising candidate due to its superior receiver sensitivity [4-7]. Considering the application scenario of PON, a number of simplified coherent architectures are proposed to reduce the cost [8]. However, most of the recent work focus on comparing received power sensitivity, and other performance metrics are not fully analyzed [8-10].

In this paper, we provide a detailed comparison of ten CD and DD schemes operating with 50Gb/s/λ non-return-to-zero (NRZ) signal through numerical simulation. Different from previous work, we investigate three levels of coherent receivers according to the cost: 1) with intensity-only simplified architecture, 2) with phase-insensitive complex reception, and 3) with both complex reception and phase recovery, respectively. Furthermore, to meet the requirement of practical implementation, the receiver power sensitivity at back-to-back (BTB), the influence of frequency offset, local oscillator (LO) power, laser linewidth, and fiber dispersion are also studied.

2. Transmitter and Receiver Structures

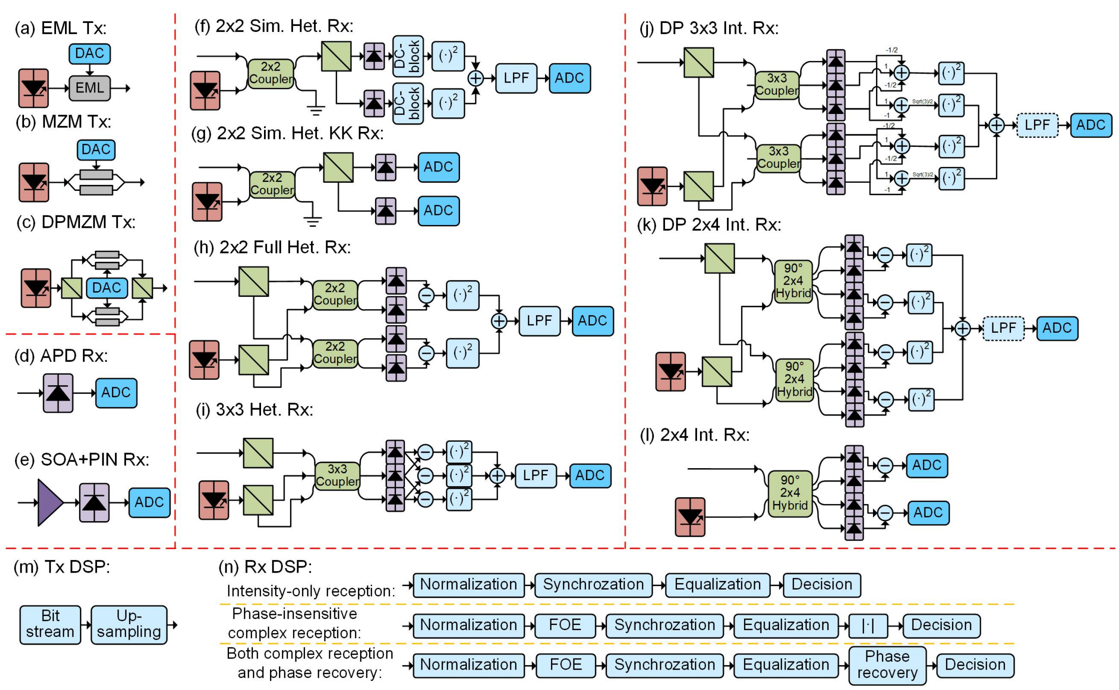

Fig. 1. Transmitter and receiver structures. DAC: digital-to-analog convertor; EML: external modulated laser; MZM: Mach-Zehnder modulator; Tx: transmitter; Rx: receiver; Sim: simplified; Het.: heterodyne; LPF: low-pass filter; ADC: analog-to-digital convertor; DP: dual-polarization; Int.: intradyne. FOE: frequency offset estimation.

Fig. 1 shows the transmitter and receiver structures for DD and CD schemes investigated in this work. At the transmitter, external modulated laser (EML) in Fig.1(a) is employed for most receivers as a low-cost solution. Mach-Zehnder modulator (MZM) in Fig.1(b), which generates BPSK instead of OOK signal, is used to combine with both phase and polarization diversity 2×4 intradyne receiver in Fig.1(k) (without square operation), in order to present the performance of both complex reception and phase recovery. In addition, dual-polarization (DP) MZM transmitter with Alamouti-coding is compared with the 2×4 intradyne receiver in Fig.1(l).

At the receiver, APD and SOA+PIN in Fig.1(d) and Fig.1(e) are tested as representative DD schemes. For heterodyne coherent receiver, single-ended detection with analog square operation architecture in Fig.1(f), single-ended detection with Kramers-Kronig relation in Fig.1(g), and balance detection with analog square operation in Fig.1(h) are taken into consideration. It should be noted that practical 2x1 coupler are realized by leaving one output of the 2×2 coupler unused. As shown in Fig.1(i), heterodyne receiver can be alternately implemented with 120° 3×3 coupler, high-order component elimination and square operation. For homodyne detection, both 120° 3×3 coupler in Fig.1(j) and 90° 2×4 hybrid in Fig.1(k) are investigated.

According to the cost after O-E frontend, the coherent receiver can be divided into three categories: intensity-only reception with square operation-based analog pre-process, phase-insensitive complex reception with ADC-only detection, and complex reception and phase recovery with ADC-only detection.

The simulation is carried out in VPItransmissionMaker^{TM}. We use 50Gbaud NRZ signal without pulse shaping for test. At the transmitter, the linewidth of transmitter laser source is set as 10MHz. The bandwidth, modulation index and chirp factor of EML are 25GHz, 0.8, and 1, respectively. At the receiver, the linewidth of LO is 10MHz. The insertion loss of 2×2 coupler, 3×3 coupler, and 2×4 hybrid are all set as 1dB for fair comparison. The PD is modeled with 35GHz bandwidth and 0.7A/W responsivity. The dark current and thermal noise are set as 3×10^{-9}A and 10^{-11} A/Hz$^{1/2}$, respectively. The frequency offset between transmitter-side laser and LO for homodyne and heterodyne detection are optimized as 0GHz and 35GHz, respectively.

3. Results and Discussions

BTB receiver sensitivity: Fig.2 displays the simulation results of DD and CD receivers at BTB. At bit-error rate (BER) of 1×10^{-2}, the sensitivity of different schemes can be sorted from the least to the most sensitive as following: class A: APD (-27.5dBm); class B: 2×2 Sim. Het., 2×2 Sim. Het. KK., 3x3 Het. (-28.8dBm); class C: SOA+PIN (-30.3dBm); class D: 3×3 DP Int., 2×4 DP Int. (-32.0dBm); class E: DPMZM+2×4 Int. (-37.5dBm); class F: MZM+2×4 DP Int. (-40.6dBm).

Results explanations: 1) Single-ended heterodyne detection has inherent 3dB sensitivity degradation since it wastes half of signal power from one of the 2×2 coupler output. 2) Complex equalization outperforms intensity-only equalization by about 2dB, because the channel response is linear in the former case. 3) MZM transmitter has higher sensitivity thanks to both removal of DC component in the signal and the increase in Euclidean distance by utilizing phase diversity. 4) Only one polarization signal can beat with LO in Alamouti-coding scheme, resulting in 3dB sensitivity penalty compared with MZM+2×4 DP intradyne receiver. 5) KK detection shows no advantage since the LO-signal power ratio is sufficiently large, so that signal-signal beat interference (SSBI) is an insignificant factor.

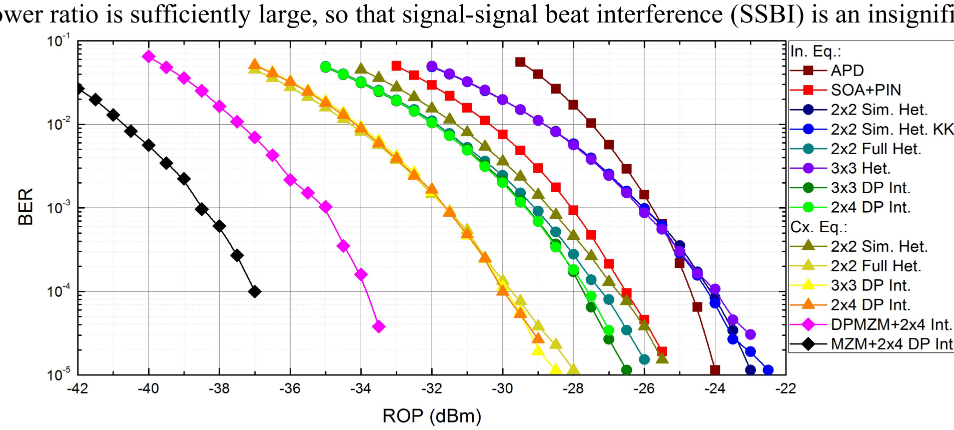

Fig.2. Simulated receiver power sensitivity of DD and CD schemes at back-to-back scenario. ROP: received optical power; In. Eq.: intensity equalization; Cx. Eq.: complex equalization.

Influence of LO power: Fig.3(a) shows the simulated sensitivity penalty versus LO power for different coherent detection receivers with intensity-only/complex equalization at BTB, respectively. At BER of 1×10^{-2}, the penalty at low LO power from smallest to largest is sorted as: class A: 3×3 Het.; class B: 2×2 Sim. Het., 2×2 Sim Het. KK, 2×2 Full Het., DPMZM+2×4 Int.; class C: 3×3 DP Int.; class D: 2×4 DP Int.; MZM+2×4 DP Int.

Results explanations: 1) The shot noise of PD is proportional to the input optical power, while thermal noise is determined by temperature. Therefore, sensitivity would gradually saturate to the shot noise limit at high LO power.

2) Coherent receiver with larger number of PDs has lower input power for each PD, and thus worse performance is caused at low LO power due to the thermal noise.

Influence of laser linewidth: Fig.3(b) shows the simulated sensitivity penalty versus transmitter-side laser linewidth for DD and CD schemes at BTB, respectively. Negligible penalty can be observed for DD and intensity-only simplified CD schemes. For MZM with 2×4 DP intradyne detection architecture, 10MHz linewidth would induce 0.5dB penalty. The results confirm the feasibility of large linewidth lasers for low-cost coherent receiver.

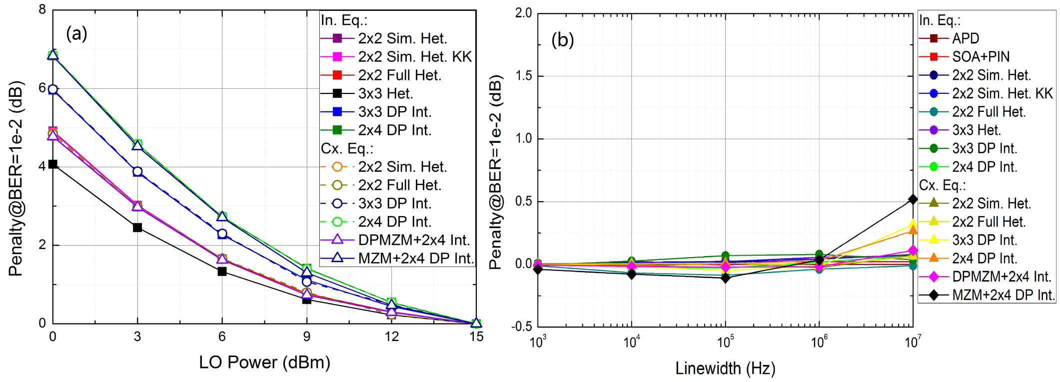

Fig.3. (a) Simulated sensitivity penalty versus LO power for different coherent detection receivers with intensity-only/complex equalization at BTB, respectively. LO: local oscillator. (b) Simulated sensitivity penalty versus transmitter-side laser linewidth for DD and coherent detection schemes at BTB, respectively.

Influence of frequency offset: Fig.4(a) shows the simulated sensitivity penalty versus frequency offset for different coherent detection receiver at BTB. For 0.5dB penalty at BER of 1×10^{-2}, the frequency interval of heterodyne detection and intradyne schemes are [-40GHz, 40GHz] and [30GHz, 50GHz], respectively. The reason is that for heterodyne detection, smaller frequency offset would result in spectral overlap, while larger frequency offset is limited by the PD bandwidth. Therefore, temperature control is an important issue if coherent receiver is chosen.

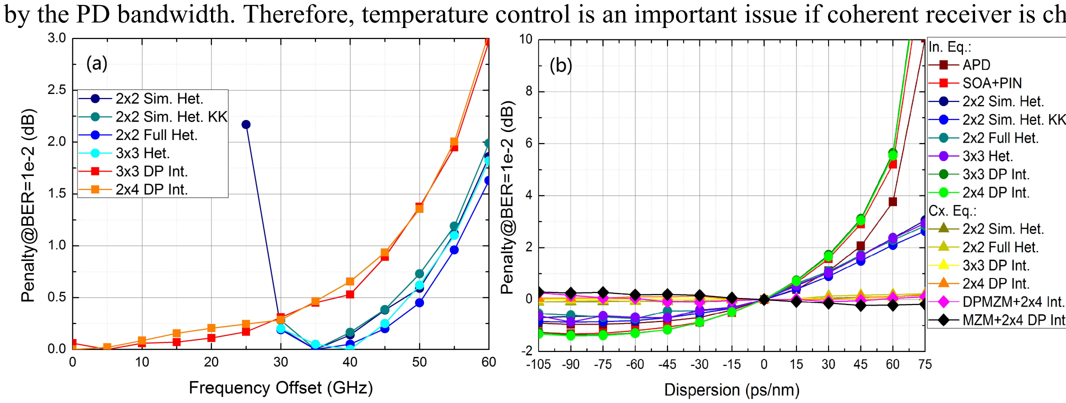

Fig.4. (a) Simulated sensitivity penalty versus frequency offset for different coherent detection receiver at BTB. (b) Simulated fiber dispersion penalty of DD and coherent detection schemes, respectively.

Influence of fiber dispersion: Fig.4(b) shows the simulated fiber dispersion penalty of DD and CD schemes, respectively. Note that the chirp factor of EML is set as 1, and only FFE is used. One can find that: 1) APD, SOA+PIN, 3×3 DP Int. (In. Eq.) and 4×4 DP Int. (In. Eq.) are severely affected by large positive dispersion. The penalty comes from the dispersion induced power fading effect, since the phase information is lost during/before PD detection. 2) In comparison, the penalty can be reduced by using heterodyne detection schemes, which avoid power fading with single-sideband configuration at PD. 3) Furthermore, if both amplitude and phase information are obtained, dispersion becomes a linear impairment and thus can be fully mitigated by complex equalization.

4. Conclusions

In this paper, we carry out a comparative study of various CD and DD schemes for 50G PON through numerical simulation. The receiver power sensitivity at BTB, the influence of frequency offset, LO power, laser linewidth, and fiber dispersion are compared. For coherent receiver, we also investigate the performance with intensity-only simplified architecture, with phase-insensitive and phase-sensitive complex reception, respectively.

5. References

[1] IEEE P802.3ca 50G-EPON Task Force.
[2] ITU-T Q2/SG15, Contribution 641, 2017.
[3] J. Zhang, J. Yu, et al., OFC2019, Th4C.3.
[4] D. van Veen, V. Houtsma, OFC2017, Th5A.4.
[5] J. Zhang, J.S.Wey, et al., ECOC2018, Tu1B.1.
[6] J. Zhang, J. Yu, et al., OFC2019, Th3F.1.
[7] M. S. Erkılınç, D. Lavery, et al., JLT, 34(8), 2016.
[8] M. S. Erkılınç, D. Lavery, et al., JLT, 36(16), 2018.
[9] A. Shahpari, R. M. Ferreira, et al., JLT, 35(4), 2017.
[10] D. Lavery, T. Gerard, et al., JOCN, 11(2), 2019.